Weierstraß–Institut
für Angewandte Analysis und Stochastik

im Forschungsverbund Berlin e.V.

Preprint ISSN 0946 – 8633

Numerical study of a stochastic particle method for homogeneous gas phase reactions

Markus Kraft[1], Wolfgang Wagner[2]

submitted: 28th March 2000

[1] Department of Chemical Engineering
University of Cambridge
Pembroke Street
Cambridge CB2 3RA, UK
E-Mail: markus_kraft@cheng.cam.ac.uk

[2] Weierstrass Institute for
Applied Analysis and Stochastics
Mohrenstrasse 39
D-10117 Berlin, Germany
E-Mail: wagner@wias-berlin.de

Preprint No. 570
Berlin 2000

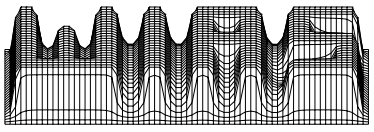

1991 Mathematics Subject Classification. 65C35, 60K40.

Key words and phrases. Stochastic particle method, combustion, convergence, efficiency.

Edited by
Weierstraß–Institut für Angewandte Analysis und Stochastik (WIAS)
Mohrenstraße 39
D — 10117 Berlin
Germany

Fax: + 49 30 2044975
E-Mail (X.400): c=de;a=d400-gw;p=WIAS-BERLIN;s=preprint
E-Mail (Internet): preprint@wias-berlin.de
World Wide Web: http://www.wias-berlin.de/

Abstract

In this paper we study a stochastic particle system that describes homogeneous gas phase reactions of a number of chemical species. First we introduce the system as a Markov jump process and discuss how relevant physical quantities are represented in terms of appropriate random variables. Then, we show how various deterministic equations, used in the literature, are derived from the stochastic system in the limit when the number of particles goes to infinity. Finally, we apply the corresponding stochastic algorithm to a toy problem, a simple formal reaction mechanism, and to a real combustion problem. This problem is given by the isothermal combustion of a homogeneous mixture of hepthane and air modelled by a detailed reaction mechanism with 107 chemical species and 808 reversible reactions. Heptane as described in this chemical mechanism serves as model-fuel for different types of internal combustion engines. In particular, we study the order of convergence with respect to the number of simulation particles, and illustrate the limitations of the method.

Contents

1. Introduction

In this paper we study a stochastic particle system that describes the homogeneous gas phase reaction process of a number of chemical species at constant pressure and temperature. The **reaction mechanism** consists of several elementary chemical reactions,

$$(\nu_{\alpha,1},\ldots,\nu_{\alpha,S}) \quad \longleftrightarrow \quad (\nu^*_{\alpha,1},\ldots,\nu^*_{\alpha,S})\,, \qquad \alpha = 1,\ldots,I\,, \tag{1.1}$$

where S is the number of chemical species and I is the number of possible reactions. The stoichiometric coefficients $\nu_{\alpha,i}$ and $\nu^*_{\alpha,i}$ of the species i in reaction α are non-negative integer values. The **time evolution** of the state variables is given by the following initial value problem (cf. [20, formulas (2), (49), (51)]; [17]),

$$\frac{dY_i}{dt} = \frac{W_i}{\varrho(Y)}\,\dot\omega_i(Y)\,, \qquad Y_i(0) = Y_{0,i}\,, \qquad i = 1,\ldots,S\,, \tag{1.2}$$

with the chemical production rate of the i-th species

$$\dot\omega_i(Y) = \sum_{\alpha=1}^{I} (\nu^*_{\alpha,i} - \nu_{\alpha,i})\, q_\alpha(Y) \tag{1.3}$$

and the rate of progress of the α-th reaction

$$q_\alpha(Y) = K_{\alpha,f} \prod_{k=1}^{S} [X_k]^{\nu_{\alpha,k}} - K_{\alpha,r} \prod_{k=1}^{S} [X_k]^{\nu^*_{\alpha,k}}\,. \tag{1.4}$$

Here Y, $[X]$ and W denote the vectors of the mass fractions, the molar concentrations, and the molecular weights of the species, respectively. The mass density is denoted by ϱ. The numbers $K_{\alpha,f}$ and $K_{\alpha,r}$ are the forward and reverse rate constants for the α-th reaction.

One of the first publications on calculating homogeneous reaction systems using stochastic ideas is Bunker et al. [5]. In this paper an algorithm was proposed to simulate the combustion of propane in an adiabatic plug flow reactor. The chemical mechanism that was used contained 17 species and 37 reactions. Independently, Gillespie suggested an algorithm that mimics the dynamics of any well stirred gas mixture of reactive chemical species in thermal equilibrium [11]. In [13] he gave a derivation of the chemical master equation proving that it is an exact description of any well stirred and thermally equilibrated gas-phase chemical system. This approach can be viewed as a mesoscopic description of chemical reactions that is between the macroscopic description, given by particle densities averaged over a control volume, and the microscopic description given by the momentum and the position of all molecules contained in the control volume. This algorithm, that will be subject of our investigations, has been applied by various authors in recent years for various purposes.

Gillespie demonstrated that the stochastic algorithm is able to account for microscopic fluctuations [12]. These fluctuations can not be captured in a deterministic approach given by a system of ordinary differential equations. This has been illustrated by studying a steady state solution of the Lotka reaction system. Similar investigation have been performed on the Brusselator and the Oregonator reaction system, the later as an idealized

model for the Belousov-Zhabotinski reactions. Other authors used Gillespie's algorithm to study polymerization reactions. For example in [2] the formation of soot using a coagulation reaction model has been investigated. Also reaction diffusion problems have been studied using Gillespie's algorithm in conjunction with an algorithm that accounts for the diffusion process. The Fisher equation was studied in [16], [3], and [4]. The Maginu equation has been investigated in [7] and a reaction-diffusion model of receptor cells was solved using a Gillespie's algorithm in [10]. Another area where the Gillespie algorithm has been extensively applied is the modelling of surface processes [9]. For example the time development of surface interfaces and adsorption-desorption phenomena have been studied in [22], surface catalysis was investigated in [18], and temperature-programmed desorption was studied in [21] and [15]. The same authors have also provided a public domain software package called chemical kinetics simulator (CKS). This package is based on the algorithm as described by Bunker et al. and Gillespie. It models homogeneous gas-phase reactions system for isothermal and adiabatic conditions [14].

The **purpose of this paper** is to study convergence and performance properties of the stochastic algorithm. In particular, the order of convergence is determined numerically, and the algorithm is applied to real combustion problems using practically relevant fuels. The paper is organized as follows. **Section 2** is concerned with the description of the stochastic model. The basic Markov jump process is defined, and relevant combustion quantities are represented in terms of related random variables. Various deterministic equations are derived from the stochastic system. Examples from the combustion literature are considered. Finally, the stochastic algorithm is described. Results of numerical experiments are presented in **Section 3**. Two test cases are considered, first a toy model from the classical paper by Gillespie, and second a practically relevant example, the combustion of heptane. For comparison, an accurate deterministic method is used. The first part of test calculations is concerned with the convergence behaviour of the algorithm. In the second part the issue of performance is studied, and limitations of the present algorithm are illustrated. Finally some conclusions are drawn in **Section 4**.

2. The stochastic model

2.1. Markov process

We consider a Markov process of the form

$$Z^{(n)}(t) = \left(N_1^{(n)}(t), \ldots, N_S^{(n)}(t)\right), \qquad t \geq 0\,, \tag{2.1}$$

where $N_j^{(n)}(t) \in \{0, 1, \ldots\}$ denotes the number of particles of type $j = 1, \ldots, S$ at time t. The number of particles at time zero,

$$n = \sum_{j=1}^{S} N_j^{(n)}(0)\,, \tag{2.2}$$

plays the role of an approximation parameter. It is assumed that

$$\lim_{n\to\infty} \frac{N_i^{(n)}(0)}{n} = \lambda_i^0\,, \qquad i = 1, \ldots, S\,, \tag{2.3}$$

for some constants λ_i^0 .

The stochastic system (2.1) is a pure jump process defined by the **generator**

$$(\mathcal{A}\Phi)(x) = \sum_{\alpha=1}^{I} \tilde{K}_\alpha(x)\Big[\Phi(J_\alpha(x)) - \Phi(x)\Big], \qquad x \in \{0,1,\ldots\}^S\,, \tag{2.4}$$

where Φ is some test function. This process performs jumps according to the **jump transformation** (cf. (1.1))

$$J_\alpha(x) = (x_1 - \nu_{\alpha,1} + \nu^*_{\alpha,1}, \ldots, x_S - \nu_{\alpha,S} + \nu^*_{\alpha,S})\,. \tag{2.5}$$

The distribution of the random jump moments is determined by the **rate functions**

$$\tilde{K}_\alpha(x) = \gamma(x)^{1-\sum_{j=1}^S \nu_{\alpha,j}}\, K_\alpha \prod_{j=1}^{S} \Big[x_j\,(x_j-1)\ldots(x_j+1-\nu_{\alpha,j})\Big]\,, \tag{2.6}$$

where $K_\alpha\,,\ \alpha = 1,\ldots,I\,,$ are reaction parameters. The function γ is either of the form

$$\gamma(x) = n\,, \tag{2.7}$$

corresponding to normalization with initial particle number (cf. (2.2)), or

$$\gamma(x) = \frac{RT}{p}\sum_{j=1}^{S} x_j\,, \tag{2.8}$$

corresponding to normalization with volume (cf. (2.11) below).

Remark 2.1 *The expression in brackets in (2.6) is defined as zero in the case* $\nu_{\alpha,j} = 0$. *The product assures that a reaction may only occur if there are enough of the corresponding particles in the system (cf. (2.5)). It is zero if* $x_j < \nu_{\alpha,j}$ *for some* $j = 1,\ldots,S$.

By definition, **mass conservation** means (cf. (2.5))

$$\sum_{j=1}^{S} W_j\, J_\alpha(x)_j = \sum_{j=1}^{S} W_j\, x_j\,. \tag{2.9}$$

This property holds provided that

$$\sum_{i=1}^{S} W_i\,\nu_{\alpha,i} = \sum_{i=1}^{S} W_i\,\nu^*_{\alpha,i}\,, \qquad \alpha = 1,\ldots,I\,.$$

The basic theoretical result concerning the Markov process (2.1) is that, under assumption (2.3),

$$\lim_{n\to\infty} \frac{N_i^{(n)}(t)}{n} = \lambda_i(t)\,, \qquad i = 1,\ldots,S\,, \quad t > 0\,, \tag{2.10}$$

(cf. [19], [8, p.454]). Later we will derive equations, which are satisfied by the limit of the stochastic process. These equations can be numerically solve by the corresponding stochastic algorithm.

Here we discuss how relevant physical quantities are represented in terms of the random variables $N_k^{(n)}(t)$, $k = 1, \ldots, S$, which correspond to the mole numbers $n_k(t)$ in the chemical literature.

The **total mole number** is

$$n(t) = \sum_{k=1}^{S} n_k(t) \quad \sim \quad \sum_{k=1}^{S} N_k^{(n)}(t)\,,$$

the **total mass** is

$$m(t) = \sum_{k=1}^{S} W_k\, n_k(t) \quad \sim \quad \sum_{k=1}^{S} W_k\, N_k^{(n)}(t)\,,$$

and the **volume** is

$$V(t) = \frac{RT}{p}\, n(t) \quad \sim \quad \frac{RT}{p} \sum_{k=1}^{S} N_k^{(n)}(t)\,. \tag{2.11}$$

Note that

$$\frac{1}{n} \sum_{k=1}^{S} N_k^{(n)}(t) \quad \stackrel{n}{\longrightarrow} \quad \sum_{k=1}^{S} \lambda_k(t) =: \tilde{n}(t)\,, \tag{2.12}$$

$$\frac{1}{n} \sum_{k=1}^{S} W_k\, N_k^{(n)}(t) \quad \stackrel{n}{\longrightarrow} \quad \sum_{k=1}^{S} W_k\, \lambda_k(t) =: \tilde{m}(t)\,, \tag{2.13}$$

and

$$\frac{1}{n} \frac{RT}{p} \sum_{j} N_j^{(n)}(t) \quad \stackrel{n}{\longrightarrow} \quad \frac{RT}{p} \sum_{k=1}^{S} \lambda_k(t) =: \tilde{V}(t) = \frac{RT}{p}\, \tilde{n}(t)\,. \tag{2.14}$$

Remark 2.2 *The quantities $n(t), m(t), V(t)$ are of physical size (large values). They are obtained from the quantities $\tilde{n}(t), \tilde{m}(t), \tilde{V}(t)$ (which are calculated using the limit functions $\lambda_i(t)$) by multiplication with the appropriate number $n(0)$. The quantities below are normalized (moderate values), and we will use the same symbols for both the physical quantities and the quantities obtained using $\lambda_i(t)$.*

The **mole fraction** of a species k is given by

$$X_k(t) = \frac{n_k(t)}{n(t)} \quad \sim \quad \frac{N_k^{(n)}(t)}{\sum_j N_j^{(n)}(t)} \quad \stackrel{n}{\longrightarrow} \quad \frac{\lambda_k(t)}{\sum_j \lambda_j(t)} = \frac{\lambda_k(t)}{\tilde{n}(t)}\,, \tag{2.15}$$

its **mass fraction** is

$$Y_k(t) = \frac{W_k\, n_k(t)}{m(t)} \quad \sim \quad \frac{W_k\, N_k^{(n)}(t)}{\sum_j W_j\, N_j^{(n)}(t)} \quad \stackrel{n}{\longrightarrow} \quad \frac{W_k\, \lambda_k(t)}{\sum_j W_j\, \lambda_j(t)} = \frac{W_k\, \lambda_k(t)}{\tilde{m}(t)}\,, \tag{2.16}$$

and the **molar concentration** is

$$[X_k](t) = \frac{n_k(t)}{V(t)} \quad \sim \quad \frac{N_k^{(n)}(t)}{\frac{RT}{p} \sum_j N_j^{(n)}(t)} \quad \stackrel{n}{\longrightarrow} \quad \frac{\lambda_k(t)}{\frac{RT}{p} \sum_j \lambda_j(t)} = \frac{\lambda_k(t)}{\tilde{V}(t)}\,. \tag{2.17}$$

The **mass density** is

$$\varrho(t) = \frac{m(t)}{V(t)} = \frac{\sum_{k=1}^S W_k\, n_k(t)}{V(t)} = \sum_{k=1}^S W_k\, [X_k](t) \;\sim\; \frac{\sum_k W_k\, N_k^{(n)}(t)}{\frac{RT}{p}\sum_j N_j^{(n)}(t)} \;\stackrel{n}{\longrightarrow}\; \frac{\tilde m(t)}{\tilde V(t)}\,. \qquad (2.18)$$

The **mean molecular weight** is

$$\overline{W}(t) = \sum_{k=1}^S W_k\, X_k(t) = \frac{1}{n(t)}\sum_{k=1}^S W_k\, n_k(t) = \frac{m(t)}{n(t)} \;\sim\; \frac{\sum_k W_k\, N_k^{(n)}(t)}{\sum_j N_j^{(n)}(t)} \;\stackrel{n}{\longrightarrow}\; \frac{\tilde m(t)}{\tilde n(t)}\,.$$

One obtains from the definitions that

$$\sum_{k=1}^S Y_k(t) = 1\,, \qquad \sum_{k=1}^S X_k(t) = 1\,, \qquad \sum_{k=1}^S [X_k](t) = \frac{n(t)}{V(t)} = \frac{p}{RT}\,.$$

Note that

$$\frac{Y_k(t)}{W_k} \;=\; \frac{X_k(t)}{\overline{W}(t)} \;=\; \frac{[X_k](t)}{\varrho(t)}\,.$$

2.2. Asymptotic behaviour

The Markov process (2.1) satisfies

$$\Phi(Z^{(n)}(t)) = \Phi(Z^{(n)}(0)) + \int_0^t (\mathcal{A}\Phi)(Z^{(n)}(s))\, ds + M^{(n)}(t)\,, \qquad t \ge 0\,, \qquad (2.19)$$

where $M^{(n)}(t)$ is a martingale term vanishing in the limit $n \to \infty$. The representation (2.19) suggests that (cf. (2.4))

$$\frac{d}{dt}\lim_{n\to\infty} \Phi(Z^{(n)}(t)) = \sum_{\alpha=1}^I \lim_{n\to\infty} \tilde K_\alpha(Z^{(n)}(t))\Big[\Phi(J_\alpha(Z^{(n)}(t))) - \Phi(Z^{(n)}(t))\Big]. \qquad (2.20)$$

Note that (cf. (2.6))

$$\tilde K_\alpha(x) = \left(\frac{\gamma(x)}{n}\right)^{1-\sum_{j=1}^S \nu_{\alpha,j}} n\, K_\alpha \prod_{j=1}^S \frac{x_j\,(x_j-1)\ldots(x_j+1-\nu_{\alpha,j})}{n^{\nu_{\alpha,j}}}\,.$$

Since according to (2.10)

$$\lim_{n\to\infty} \frac{N_j^{(n)}(t)\,(N_j^{(n)}(t)-1)\ldots(N_j^{(n)}(t)+1-\nu_{\alpha,j})}{n^{\nu_{\alpha,j}}} = \lambda_j(t)^{\nu_{\alpha,j}}\,,$$

one obtains from (2.20) the equation

$$\frac{d}{dt}\lim_{n\to\infty} \Phi(Z^{(n)}(t)) = \qquad (2.21)$$
$$\sum_{\alpha=1}^I \tilde\gamma(t)^{1-\sum_{j=1}^S \nu_{\alpha,j}}\, K_\alpha \lim_{n\to\infty} n\Big[\Phi(J_\alpha(Z^{(n)}(t))) - \Phi(Z^{(n)}(t))\Big] \prod_{j=1}^S \lambda_j(t)^{\nu_{\alpha,j}},$$

where the notation

$$\tilde{\gamma}(t) \;=\; \lim_{n\to\infty} \frac{1}{n}\,\gamma(Z^{(n)}(t))$$

has been used. Note that

$$\tilde{\gamma}(t) = 1\,, \tag{2.22}$$

in case (2.7), and

$$\tilde{\gamma}(t) = \tilde{V}(t)\,, \tag{2.23}$$

in case (2.8) (cf. (2.14)).

Choosing appropriate test functions Φ allows us to derive equations for the limiting functions $\lambda_k(t)$ from (2.10) as well as for the quantities (2.15)-(2.17).

Consider the test functions

$$\Phi_i(x) = \frac{W_i\, x_i}{\sum_{j=1}^S W_j\, x_j}\,, \qquad i = 1, \ldots, S\,,$$

and note that (cf. (2.16))

$$\lim_{n\to\infty} \Phi_i(Z^{(n)}(t)) = \frac{W_i\,\lambda_i(t)}{\sum_{j=1}^S W_j\,\lambda_j(t)} = Y_i(t)\,.$$

According to (2.9) one obtains

$$\Big[\Phi_i(J_\alpha(x)) - \Phi_i(x)\Big] = \\ \frac{1}{\sum_{j=1}^S W_j\, x_j}\Big[W_i\,(x_i - \nu_{\alpha,i} + \nu^*_{\alpha,i}) - W_i\, x_i\Big] = \frac{1}{\sum_{j=1}^S W_j\, x_j}\Big[W_i\,(\nu^*_{\alpha,i} - \nu_{\alpha,i})\Big]$$

so that (cf. (2.13))

$$\lim_{n\to\infty} n\Big[\Phi_i(J_\alpha(Z^{(n)}(t))) - \Phi_i(Z^{(n)}(t))\Big] = \frac{1}{\tilde{m}(t)}\Big[W_i\,(\nu^*_{\alpha,i} - \nu_{\alpha,i})\Big],$$

and equation (2.21) takes the form

$$\frac{d}{dt}\,Y_i(t) = \frac{W_i}{\tilde{m}(t)} \sum_{\alpha=1}^I \tilde{\gamma}(t)^{1-\sum_{j=1}^S \nu_{\alpha,j}}\, K_\alpha\,[\nu^*_{\alpha,i} - \nu_{\alpha,i}] \prod_{j=1}^S \lambda_j(t)^{\nu_{\alpha,j}}\,. \tag{2.24}$$

Consider the test functions

$$\Phi_i(x) = \frac{x_i}{n}\,, \qquad i = 1, \ldots, S\,,$$

and note that (cf. (2.10))

$$\lim_{n\to\infty} \Phi_i(Z^{(n)}(t)) = \lambda_i(t)\,.$$

According to (2.5) one obtains

$$n\Big[\Phi_i(J_\alpha(x)) - \Phi_i(x)\Big] = \nu^*_{\alpha,i} - \nu_{\alpha,i}\,,$$

and equation (2.21) takes the form

$$\frac{d}{dt}\,\lambda_i(t) = \sum_{\alpha=1}^{I} \tilde\gamma(t)^{1-\sum_{j=1}^S \nu_{\alpha,j}}\, K_\alpha\,[\nu^*_{\alpha,i} - \nu_{\alpha,i}] \prod_{j=1}^{S} \lambda_j(t)^{\nu_{\alpha,j}}\,, \qquad i = 1,\dots,S\,. \tag{2.25}$$

Consider the test functions

$$\Phi_i(x) = \frac{x_i}{\sum_{j=1}^S x_j}\,, \qquad i = 1,\dots,S\,,$$

and note that (cf. (2.15))

$$\lim_{n\to\infty} \Phi_i(Z^{(n)}(t)) = \frac{\lambda_i(t)}{\sum_{j=1}^S \lambda_j(t)} = X_i(t)\,.$$

According to (2.5) one obtains

$$\begin{aligned}
\Phi_i(J_\alpha(x)) - \Phi_i(x) &= \frac{x_i + \nu^*_{\alpha,i} - \nu_{\alpha,i}}{\sum_{j=1}^S x_j + \sum_{j=1}^S[\nu^*_{\alpha,j} - \nu_{\alpha,j}]} - \frac{x_i}{\sum_{j=1}^S x_j} \\
&= \frac{\Big(\nu^*_{\alpha,i} - \nu_{\alpha,i}\Big)\Big(\sum_{j=1}^S x_j\Big) - x_i\,\sum_{j=1}^S[\nu^*_{\alpha,j} - \nu_{\alpha,j}]}{\Big(\sum_{j=1}^S x_j\Big)\Big(\sum_{j=1}^S x_j + \sum_{j=1}^S[\nu^*_{\alpha,j} - \nu_{\alpha,j}]\Big)} \\
&= \frac{\nu^*_{\alpha,i} - \nu_{\alpha,i}}{\sum_{j=1}^S x_j + \sum_{j=1}^S[\nu^*_{\alpha,j} - \nu_{\alpha,j}]} - \frac{x_i\,\sum_{j=1}^S[\nu^*_{\alpha,j} - \nu_{\alpha,j}]}{\Big(\sum_{j=1}^S x_j\Big)\Big(\sum_{j=1}^S x_j + \sum_{j=1}^S[\nu^*_{\alpha,j} - \nu_{\alpha,j}]\Big)}
\end{aligned}$$

so that (cf. (2.12))

$$\lim_{n\to\infty} n\Big[\Phi_i(J_\alpha(Z^{(n)}(t))) - \Phi_i(Z^{(n)}(t))\Big] = \frac{\nu^*_{\alpha,i} - \nu_{\alpha,i}}{\tilde n(t)} - \frac{\lambda_i(t)\,\sum_{j=1}^S[\nu^*_{\alpha,j} - \nu_{\alpha,j}]}{\tilde n(t)^2}.$$

Thus, equation (2.21) takes the form

$$\frac{d}{dt}\,X_i(t) = \sum_{\alpha=1}^{I} \tilde\gamma(t)^{1-\sum_{j=1}^S \nu_{\alpha,j}}\, K_\alpha\, \frac{[\nu^*_{\alpha,i} - \nu_{\alpha,i}]\,\tilde n(t) \;-\; \lambda_i(t)\,\sum_{j=1}^S[\nu^*_{\alpha,j} - \nu_{\alpha,j}]}{\tilde n(t)^2} \prod_{j=1}^{S} \lambda_j(t)^{\nu_{\alpha,j}}\,.$$

2.3. Examples

With the choice (2.8), equation (2.24) takes the form (cf. (2.23), (2.17), (2.18))

$$\frac{d}{dt}\,Y_i(t) = \frac{W_i}{\varrho(t)} \sum_{\alpha=1}^{I} K_\alpha\,[\nu^*_{\alpha,i} - \nu_{\alpha,i}] \left(\prod_{j=1}^{S} [X_j](t)^{\nu_{\alpha,j}}\right), \qquad i = 1,\dots,S\,.$$

Considering reverse reactions explicitly one obtains the equation

$$\begin{aligned}\frac{d}{dt}Y_i(t) &= \frac{W_i}{\varrho(t)}\sum_{\alpha=1}^{I} K_{\alpha,f}\,[\nu^*_{\alpha,i}-\nu_{\alpha,i}]\left(\prod_{j=1}^{S}[X_j](t)^{\nu_{\alpha,j}}\right)\\ &\quad+\frac{W_i}{\varrho(t)}\sum_{\alpha=1}^{I} K_{\alpha,r}\,[\nu_{\alpha,i}-\nu^*_{\alpha,i}]\left(\prod_{j=1}^{S}[X_j](t)^{\nu^*_{\alpha,j}}\right)\\ &= \frac{W_i}{\varrho(t)}\sum_{\alpha=1}^{I}[\nu^*_{\alpha,i}-\nu_{\alpha,i}]\left(K_{\alpha,f}\prod_{j=1}^{S}[X_j](t)^{\nu_{\alpha,j}}-K_{\alpha,r}\prod_{j=1}^{S}[X_j](t)^{\nu^*_{\alpha,j}}\right),\end{aligned}$$

which is identical with **equation (1.2)**.

Example 2.3 *In the example in [8, p.454] rate functions of the form (2.6) are considered with γ as in (2.7) and*

$$K_\alpha = \frac{\mu_\alpha}{\prod_{k=1}^{S}\nu_{\alpha,k}!}\,. \tag{2.26}$$

The corresponding equation is obtained from equation (2.25) (cf. (2.22)),

$$\frac{d}{dt}\lambda_i(t) = \sum_{\alpha=1}^{I} K_\alpha\,[\nu^*_{\alpha,i}-\nu_{\alpha,i}]\prod_{j=1}^{S}\lambda_j(t)^{\nu_{\alpha,j}}\,,\qquad i=1,\ldots,S\,. \tag{2.27}$$

Remark 2.4 *The number of possible choices of the corresponding particle combination is $\frac{x_j\,(x_j-1)\ldots(x_j+1-\nu_{\alpha,j})}{\nu_{\alpha,j}\,!}$. In particular, there is only one choice in the case $x_j=\nu_{\alpha,j}$. This suggests that the factor $\nu_{\alpha,j}\,!$ should be included in K_α as shown in (2.26).*

Remark 2.5 *Note that the behaviour of the process, and therefore its limits, depend on the choice of the normalizing factor γ, and of the reaction parameters K_α.*

Example 2.6 *We consider the example from [11, p. 422]. There are $S=4$ species named A,B,C,D and $I=6$ reactions described by*

$$\begin{aligned}B\to C \quad&\sim\quad \nu_1=(0,1,0,0)\,,\quad \nu^*_1=(0,0,1,0)\,,\\ C\to B \quad&\sim\quad \nu_2=(0,0,1,0)\,,\quad \nu^*_2=(0,1,0,0)\,,\\ 2B\to D \quad&\sim\quad \nu_3=(0,2,0,0)\,,\quad \nu^*_3=(0,0,0,1)\,,\\ D\to 2B \quad&\sim\quad \nu_4=(0,0,0,1)\,,\quad \nu^*_4=(0,2,0,0)\,,\\ A+B\to 2B \quad&\sim\quad \nu_5=(1,1,0,0)\,,\quad \nu^*_5=(0,2,0,0)\,,\\ 2B\to A+B \quad&\sim\quad \nu_6=(0,2,0,0)\,,\quad \nu^*_6=(1,1,0,0)\,.\end{aligned}$$

From (2.6), with with γ as in (2.7) and K_α as in (2.26), one obtains the rate functions

$$\begin{aligned}\tilde K_1(x) &= \mu_1\,x_2\,,\qquad \tilde K_2(x)=\mu_2\,x_3\,,\qquad \tilde K_3(x)=n^{-1}\,\frac{\mu_3}{2}\,x_2\,(x_2-1)\,,\\ \tilde K_4(x) &= \mu_4\,x_4\,,\qquad \tilde K_5(x)=n^{-1}\,\mu_5\,x_1\,x_2\,,\qquad \tilde K_6(x)=n^{-1}\,\frac{\mu_6}{2}\,x_2\,(x_2-1)\,.\end{aligned}$$

The corresponding limiting equation takes the form (cf. (2.27))

$$\begin{aligned}
\frac{d}{dt}\,\lambda_1(t) &= -\mu_5\,\lambda_1(t)\,\lambda_2(t) + \frac{\mu_6}{2}\,\lambda_2(t)^2\,,\\
\frac{d}{dt}\,\lambda_2(t) &= -\mu_1\,\lambda_2(t) + \mu_2\,\lambda_3(t) - \mu_3\,\lambda_2(t)^2 + 2\,\mu_4\,\lambda_4(t) + \mu_5\,\lambda_1(t)\,\lambda_2(t) - \frac{\mu_6}{2}\,\lambda_2(t)^2\,,\\
\frac{d}{dt}\,\lambda_3(t) &= \mu_1\,\lambda_2(t) - \mu_2\,\lambda_3(t)\,,\\
\frac{d}{dt}\,\lambda_4(t) &= \frac{\mu_3}{2}\,\lambda_2(t)^2 - \mu_4\,\lambda_4(t)\,,
\end{aligned}$$

which coincides with formulas (34a-d) in [11, p.422].

2.4. Description of the algorithm

The stochastic algorithm for the numerical treatment of equation (1.2)-(1.4) consists in generating trajectories of the Markov process (2.1) and averaging the appropriate functionals.

Given the state

$$x = \left(N_1^{(n)}(t), \ldots, N_S^{(n)}(t)\right), \qquad t \geq 0\,,$$

the process remains there for a random time τ having exponential distribution with the **waiting time parameter** (cf. (2.6))

$$\pi(x) = \sum_{\alpha=1}^{I} \tilde{K}_\alpha(x)\,,$$

i.e.

$$\mathrm{Prob}(\tau \geq s) = \exp(-s\,\pi(x))\,, \qquad s \geq 0\,.$$

At the moment $t+\tau$, a particular reaction is chosen according to the **reaction probabilities**

$$p_\alpha(x) = \frac{\tilde{K}_\alpha(x)}{\pi(x)}\,, \qquad \alpha = 1, \ldots, I\,,$$

where (cf. (2.6), (2.8))

$$\tilde{K}_\alpha(x) = \left(\frac{RT}{p}\sum_{j=1}^{S} x_j\right)^{1-\sum_{j=1}^{S}\nu_{\alpha,j}} K_\alpha \prod_{j=1}^{S}\Big[x_j\,(x_j-1)\ldots(x_j+1-\nu_{\alpha,j})\Big].$$

Finally, the process jumps into the state $J_\alpha(x)$ (cf. (2.5)), and the same procedure is repeated.

3. Numerical experiments

3.1. Description of the test cases

Here we introduce the examples, which are used for studying the stochastic algorithm. The figures were obtained using the deterministic method described below in subsection 3.3. The corresponding curves will be used as reference solutions.

The **first test case** that we shall study is Example 2.6. The initial conditions are

$$X_{\mathrm{A}}(0) = 1.0\,, \quad X_{\mathrm{B}}(0) = X_{\mathrm{C}}(0) = X_{\mathrm{D}}(0) = 0\,.$$

Temperature and pressure are set to $T = 1500\,\mathrm{K}$ and $p = 1.01325\,\mathrm{PA}$. The calculations are performed in the time interval $[0, 2.0 \times 10^5]s$. The time evolution of the species' mole fractions and of density is displayed in **Figure 1**.

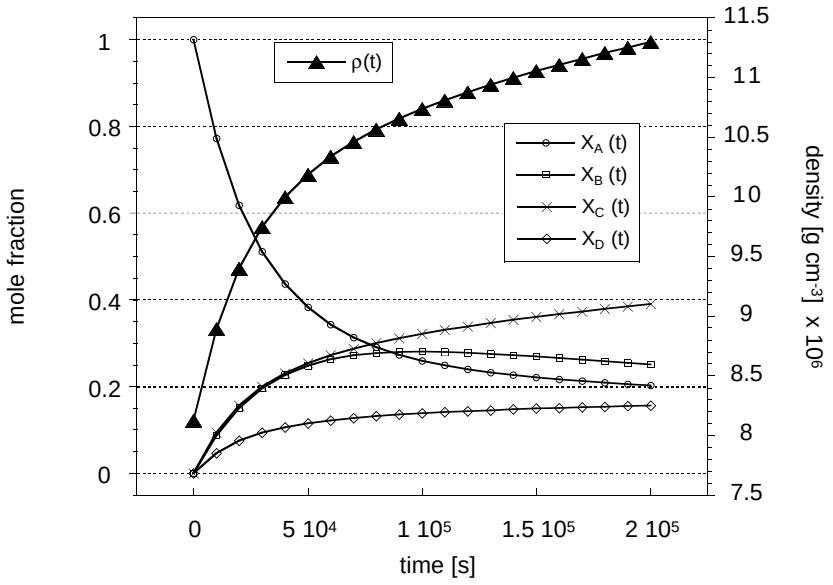

Figure 1: *Time evolution of the species' mole fractions and density.*

The **second test case** is the combustion of n-heptane. This example is of practical relevance. n-Heptane serves as primary reference fuel for internal combustion engines such as spark-ignition, diesel, and gas turbine engines. The chemistry is described by a reaction mechanism containing 107 chemical species and 808 reversible reactions [6]. The initial conditions are

$$X_{\mathrm{n-C_7H_{16}}}(0) = 0.0187\,, \quad X_{\mathrm{O_2}}(0) = 0.2061\,, \quad X_{\mathrm{N_2}}(0) = 0.7752\,.$$

Temperature and pressure are set to $T = 1500\,\mathrm{K}$ and $p = 1.01325\,\mathrm{PA}$. The time profiles of reactants and products as well as density are displayed in **Figures 2** on a short time interval and in **Figure 3** on a longer time interval. The oxidation of n-heptane takes place in several steps. In a first phase n-heptane is decomposed into smaller hydrocarbons. After

$3.0 \times 10^{-5} s$ this process is completed. At about $3.0 \times 10^{-4} s$ ignition takes place and CO is converted to CO_2. During this ignition process the number of reactions that take place increases rapidly due to a chain-branching reaction mechanism. As consequence radicals like OH and H are released. At the ignition point their mole-fraction reaches a maximum of 0.004 and 0.008 respectively.

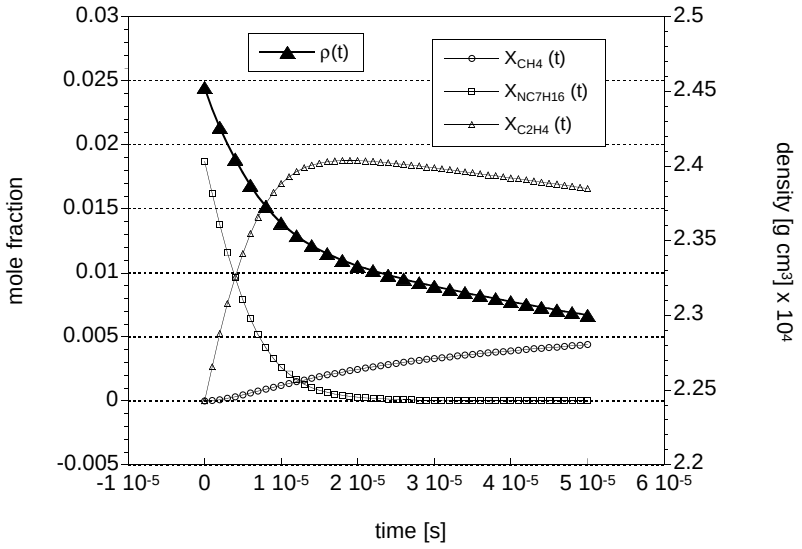

Figure 2: *Time evolution of the species' mole fractions and density.*

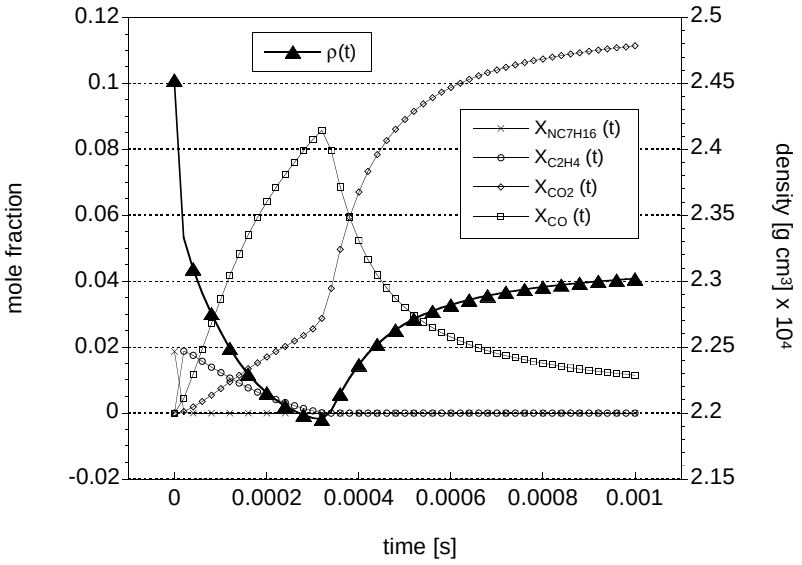

Figure 3: *Time evolution of the species' mole fractions and density.*

3.2. Confidence intervals and statistical error bound

Here we introduce some definitions and notations that are helpful for the understanding of stochastic numerical procedures.

Typical macroscopic quantities as species mole fractions and the mass density (cf. (2.15), (2.18)) are functionals of the form

$$F(t) = \Phi(n_1(t), ..., n_S(t)) \,. \tag{3.1}$$

These functionals are approximated (as $n \to \infty$) by the random variable

$$\xi^{(n)}(t) = \Phi(N_1^{(n)}(t), ..., N_S^{(n)}(t)) \,, \tag{3.2}$$

where $N_1^{(n)}, ..., N_S^{(n)}$ is the particle number model (2.1).

In order to estimate the expectation and the random fluctuations of the estimator (3.2), a number L of independent ensembles of particles is generated. The corresponding values of the random variable are denoted by $\xi^{(n,1)}(t), \ldots, \xi^{(n,L)}(t)$. The **empirical mean value** of the random variable (3.2) is defined as

$$\eta_1^{(n,L)}(t) = \frac{1}{L} \sum_{l=1}^{L} \xi^{(n,l)}(t) \,. \tag{3.3}$$

The variance of the random variable (3.2) satisfies

$$\operatorname{Var} \xi^{(n)}(t) := E\left[\xi^{(n)}(t) - E\xi^{(n)}(t)\right]^2 = E\left[\xi^{(n)}(t)\right]^2 - \left[E\xi^{(n)}(t)\right]^2$$

and is estimated by the **empirical variance** defined as

$$\eta_2^{(n,L)}(t) = \frac{1}{L} \sum_{l=1}^{L} \left[\xi^{(n,l)}(t)\right]^2 - \left[\eta_1^{(n,L)}(t)\right]^2 .$$

The empirical mean (3.3) is used to approximate the macroscopic quantity (3.1). The error of this approximation is denoted as

$$e^{(n,L)} = |\eta_1^{(n,L)}(t) - F(t)|$$

and consists of the following two components. The **systematic error** is the difference between the mathematical expectation of the random variable (3.2) and the exact value of the functional, i.e.

$$e_{sys}^{(n)}(t) = E\xi^{(n)}(t) - F(t) \,. \tag{3.4}$$

The **statistical error** is the difference between the empirical mean value and the expected value of the random variable, i.e.

$$e_{stat}^{(n,L)}(t) = \eta_1^{(n,L)}(t) - E\xi^{(n)}(t) \,.$$

Note that the random variable

$$\frac{\eta_1^{(n,L)}(t) - E\xi^{(n)}(t)}{\sqrt{\operatorname{Var} \eta_1^{(n,L)}(t)}}$$

has asymptotically (e.g., for $L \geq 50$) a standard normal distribution, as a consequence of the central limit theorem. Thus, one obtains

$$\text{Prob}\left\{\frac{\left|\eta_1^{(n,L)}(t) - E\xi^{(n)}(t)\right|}{\sqrt{\text{Var}\,\eta_1^{(n,L)}(t)}} \leq a_p\right\} \quad \sim \quad p\,, \qquad p \in (0,1)\,, \tag{3.5}$$

where the value of a_p is determined from statistical tables. Note that

$$\text{Var}\,\eta_1^{(n,L)}(t) = \frac{1}{L}\,\text{Var}\,\xi^{(n)}(t) \quad \sim \quad \frac{1}{L}\,\eta_2^{(n,L)}(t)\,. \tag{3.6}$$

From (3.5), (3.6) a **confidence interval** for the expectation of the random variable $\xi^{(n)}(t)$ is obtained as

$$I_p = \left[\eta_1^{(n,L)}(t) - a_p\sqrt{\frac{\eta_2^{(n,L)}(t)}{L}}\,,\, \eta_1^{(n,L)}(t) + a_p\sqrt{\frac{\eta_2^{(n,L)}(t)}{L}}\right],$$

where p is called the **confidence level**. This means that

$$\text{Prob}\left\{E\xi^{(n)}(t) \in I_p\right\} = \text{Prob}\left\{|e_{stat}^{(n,L)}(t)| \leq a_p\sqrt{\frac{\eta_2^{(n,L)}(t)}{L}}\right\} \quad \sim \quad p\,.$$

Thus, the value

$$c_p^{(n,L)}(t) = a_p\sqrt{\frac{\eta_2^{(n,L)}(t)}{L}}$$

is a probabilistic upper bound for the statistical error.

For the numerical studies throughout this paper a confidence level of $p = 0.999$ with $a_p = 3.29$ is used.

In order to describe the statistical error in $[0,T]$ we split this time interval in M equidistant subintervals of length Δt according the discretization

$$t_i = i\,\Delta t\,, \qquad i = 0,1,...,M\,,$$

with $t_M = T$ and use the quantity

$$c_{stat} = \max_i\left\{c_p^{(n,L)}(t_i)\right\} \tag{3.7}$$

as a measure for the statistical error.

3.3. Comparison with a deterministic numerical method

For studying the systematic error (3.4) of the stochastic algorithm, we use the comparison of the empirical mean value (3.3) with an approximation $\zeta(t)$ of the corresponding macroscopic quantity $F(t)$ obtained from an accurate deterministic numerical method. The error of this approximation is denoted as

$$e_{DASSL} = |\zeta(t) - F(t)| \,. \tag{3.8}$$

The approximation $\zeta(t)$ is obtained from the code DASSL [1]. DASSL is a code for solving systems of differential/algebraic systems. DASSL has been applied successfully to combustion problems as part of the software package SENKIN [20]. This Fortran computer program computes the time evolution of a homogeneous reacting gas mixture as described by equation (1.2). The program runs in conjunction with the CHEMKIN [17] package that facilitates the description of elementary gas-phase kinetics. The Appendix contains the chemical mechanism and the thermodynamic data for Example 2.6 in CHEMKIN format. The reaction mechanism and thermodynamic data for n-heptane oxidation were provided in CHEMKIN format also.

DASSL is based on an implicit discretization of the time derivative and a Newton method for solving the resulting nonlinear system of equations. The accuracy of DASSL is determined by two tolerances RTOL and ATOL. If m the number of significant digits required for $\zeta(t)$ then RTOL has to be set RTOL $= 10^{-(m+1)}$ and ATOL has to be set to a value at which $|F(t)|$ is essentially insignificant. For the numerical calculations in this paper the tolerances are set to RTOL $= 10^{-10}$ and ATOL $= 10^{-20}$. From that we obtain an upper bound for the deterministic error (3.8)

$$e_{\mathrm{DASSL}} \leq 10^{-8} |F(t)| \,.$$

The error

$$\tilde{e}^{(n,L)}(t) = |\eta_1^{(n,L)}(t) - \zeta(t)| \tag{3.9}$$

is a good approximation of the true error $e^{(n,L)}(t)$ for the choice of parameters in this paper. In order to get an expression for (3.9) on $[0,T]$ we calculate the quantity

$$c_{tot} = \frac{1}{M+1} \sum_{i=0}^{M} \tilde{e}^{(n,L)}(t_i) \,. \tag{3.10}$$

The error c_{tot} is an estimate for the average error in the time interval $[0,T]$.

3.4. Convergence behaviour

The errors c_{stat} and c_{tot} (cf. (3.7), (3.10)) are calculated for the **mass density** (2.18). The mass density was chosen because it is a function of all macroscopic quantities and therefore the errors c_{stat} and c_{tot} can be regarded as representative for all state variables. Tables 1-3 contain results of the numerical study. Here t_{sr} denotes the CPU time (in seconds) needed for a single run. All numerical simulation runs have been performed on a Silicon Graphics Origin 2000 work station.

Table 1 contains the results of the numerical study for the **first test case** described in Section 3.1. In this study the product $n \times L$ is constant at a value of 2.5×10^8.

Table 1: *Computational study for Gillespie mechanism*

n	$c_{stat} \times 10^{10}$	$c_{tot} \times 10^{10}$	t_{sr}	$t_{sr}/n \times 10^5$
25	9.78	564	0.0010	4.0
50	9.74	297	0.0017	3.4
100	9.70	157	0.0032	3.2
200	9.67	77.7	0.0061	3.0
400	9.67	38.5	0.012	3.0
800	9.66	17.6	0.023	2.9
1600	9.67	7.81	0.046	2.9
3200	9.66	4.25	0.093	2.9

Figure 4 displays numerical solution of the stochastic method for different particle numbers, as described in Table 1, and the numerical solution obtained from DASSL. One can see that the exact solution is covered by the confidence band for sufficiently large n.

As long as the systematic error is larger than the statistical error we can estimate the **order of convergence**. The logarithm of the error c_{tot} as given in Table 1 is printed as a function of the logarithm of the particle number in **Figure 5**. The error is compared with the slope $\frac{1}{n}$. Confidence intervals are obtained using the statistical error bound $(e_{\text{sys}} \pm e_{\text{stat}})$.

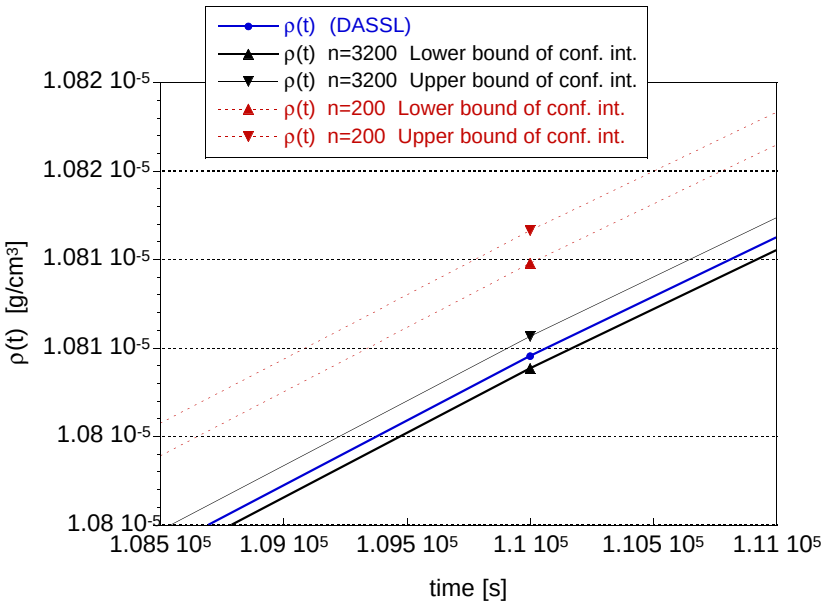

Figure 4: *Confidence intervals for the mass density corresponding to* $n = 200$ *and* $n = 3200$ *in Table 1.*

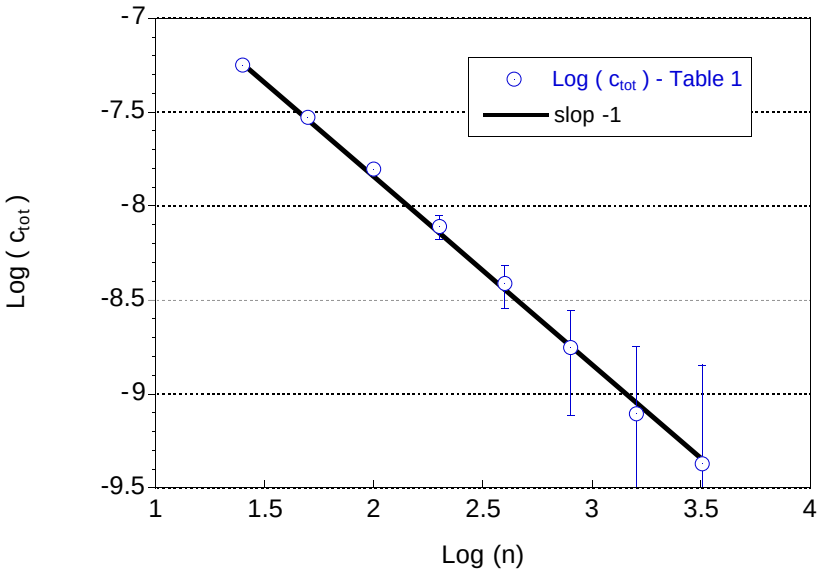

Figure 5: *Order of convergence in the first test case*

Tables 2, 3 contain the results of the numerical study for the **second test case** described in Section 3.1. The product $L \times n$ is approximately 10^6 in both tables.

Table 2: *Computational study for Heptane mechanism (starting phase)*

n	$c_{stat} \times 10^9$	$c_{tot} \times 10^9$	t_{sr}	$t_{sr}/n \times 10^4$
800	66.3	452	0.57	7.0
1200	71.5	291	0.78	6.5
1600	74.7	230	0.99	6.1
2400	76.7	184	1.4	5.8
3200	78.7	141	1.8	5.6
4800	81.3	79.9	2.7	5.5
6400	80.6	70.7	3.7	5.7
9600	81.8	48.9	5.2	5.4
12800	84.7	54.4	7.2	5.6
19200	84.6	25.5	10	5.4
25600	84.3	22.7	14	5.5
51200	81.1	30.1	28	5.5
102400	80.9	14.0	56	5.5

Table 3: *Computational study for Heptane mechanism (after ignition)*

n	$c_{stat} \times 10^9$	$c_{tot} \times 10^9$	t_{sr}	$t_{sr}/n \times 10^3$
1000	476	3932	3.1	3.6
1799	603	2856	7.6	4.2
3247	621	1675	16.3	5.0
5848	641	710	32.6	5.5
10527	698	356	58.7	5.6
19231	810	279	110	5.7
34483	710	138	198	5.7

The error c_{tot} as given in Tables 2, 3 is displayed in logarithmic scale as a function of the particle number in **Figures 6, 7**. The error is compared with the slope $\frac{1}{n}$. Due to the complexity of the second test case the order of convergence is more difficult to detect. Note that inside the confidence interval the error fluctuates.

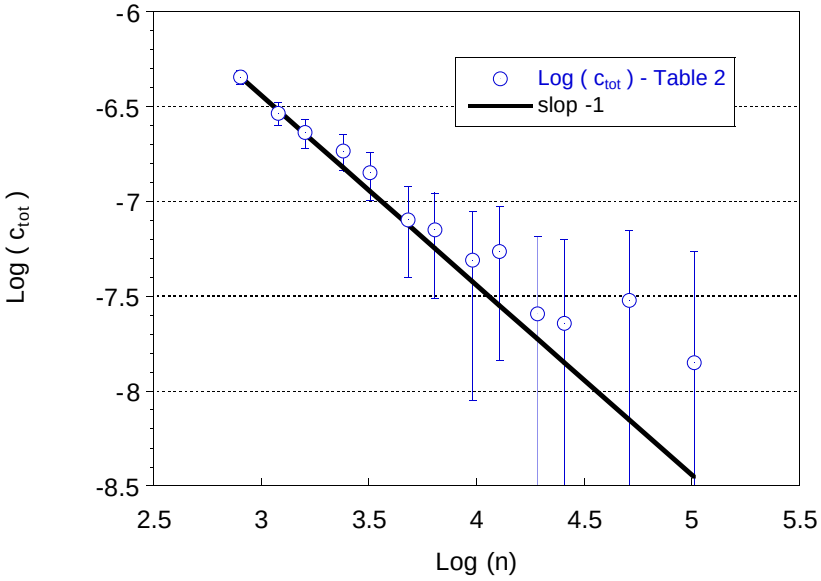

Figure 6: *Order of convergence for Table 2*

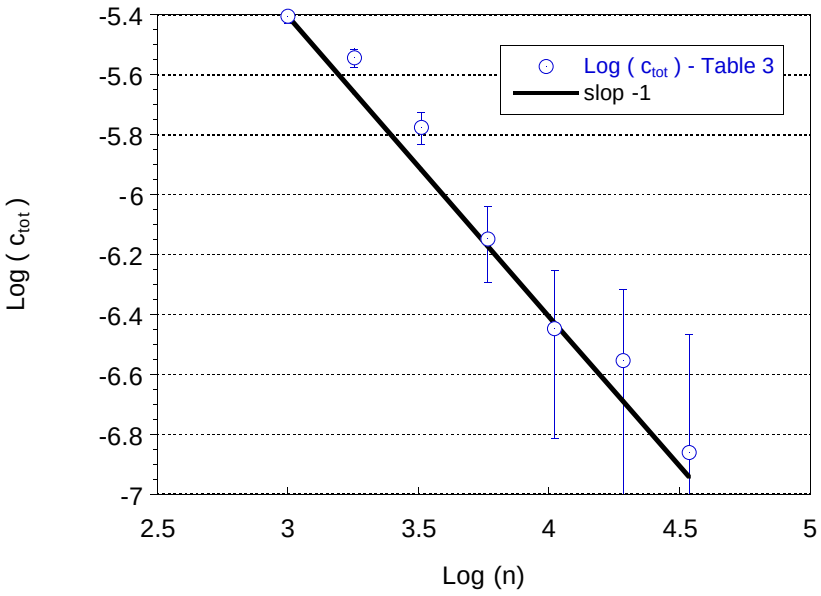

Figure 7: *Order of convergence for Table 3*

3.5. Performance and limitations

Here we discuss the issue of efficiency for the stochastic algorithm. In particular, we address the problem of **comparison with the deterministic algorithm**. We also indicate the limitations of the present stochastic method.

The CPU time for a single run of the stochastic algorithm is given in **Figure 8** (first test case) and **Figure 9** (second test case), for varying simulation time intervals and particle numbers in comparison to DASSL.

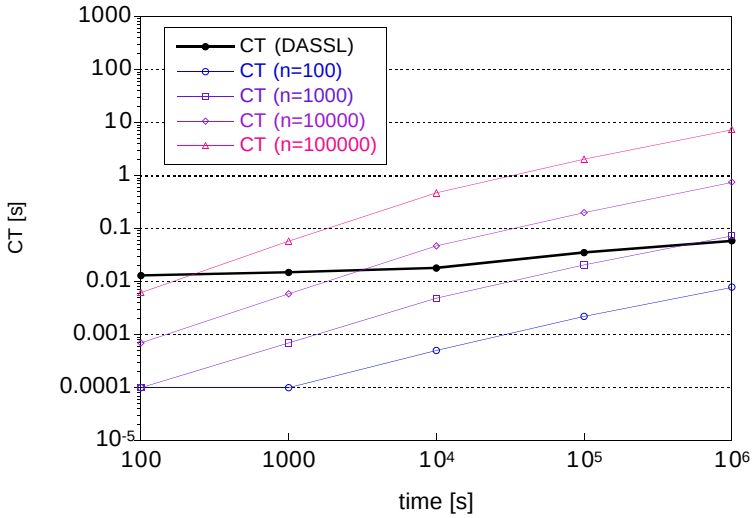

Figure 8: *CPU time for the first test case*

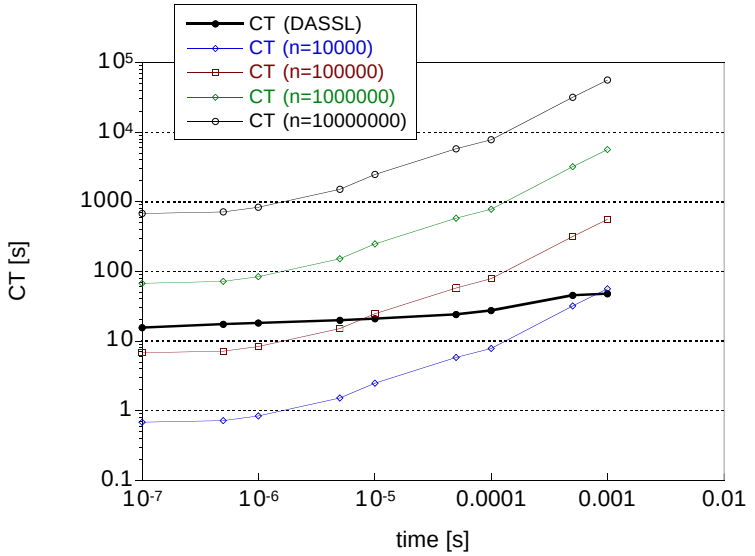

Figure 9: *CPU time for the second test case*

Concerning **computation time** $\mathrm{CT}(n,t)$, one expects the property

$$\lim_{n\to\infty} \frac{\mathrm{CT}(n,t)}{n} \quad = \quad b(t)\,. \tag{3.11}$$

This is supported by the last columns in the tables of section 3.4., and by the measured curves in Figure 8. Property (3.11) allow us to obtain curves for the computing time for different n on the basis of one measured curve. Accordingly, only the curve for $n = 10^4$ in Figure 9 was measured, while the others were calculated.

In addition, we consider the **mean number of individual reactions** $\mathrm{RN}(n,t)$ occuring in the stochastic algorithm. We illustrate for the two test cases that

$$\lim_{n\to\infty} \frac{\mathrm{RN}(n,t)}{n} \quad = \quad a(t)\,.$$

The corresponding curves are shown in **Figures 10, 11** for both test cases.

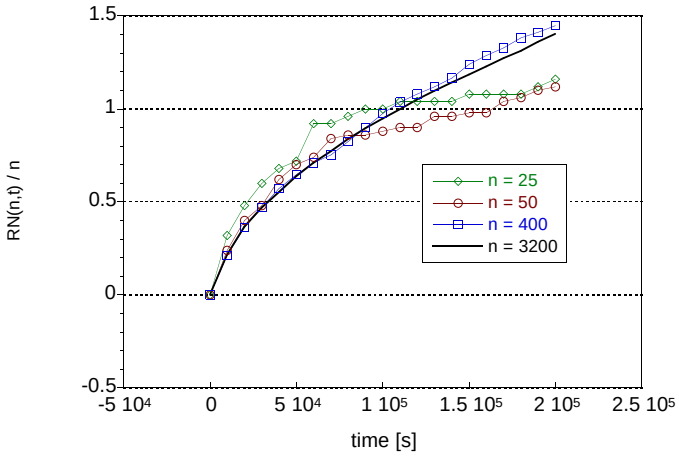

Figure 10: *Number of reactions in the first test case*

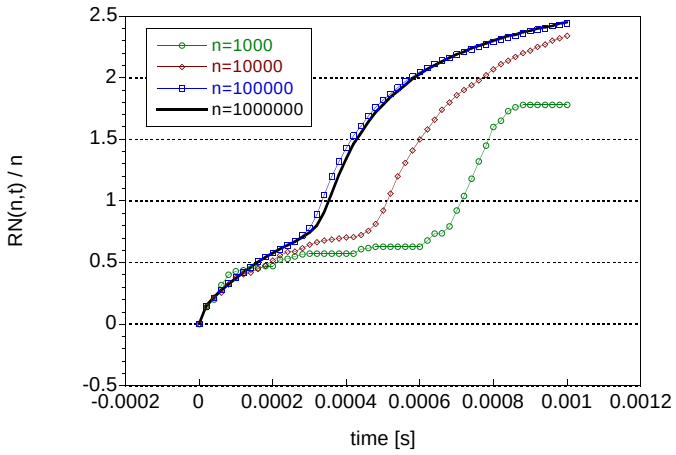

Figure 11: *Number of reactions in the second test case*

If the expression $\frac{b(t)}{a(t)}$ (mean effort per reaction) does not vary significantly in time, than the number of reactions (which is simpler to measure) can be used to estimate the actual computation time.

Figures 8 and 9 provide a quantitative illustration of the general statement that, if less accuracy is needed, the stochastic method is significantly faster than the deterministic algorithm. To make a concrete comparison in our test cases, we have first to decide which precision is necessary to catch the important features of the process. Considering the **curves for the averages** shows for which n acceptable results are obtained. These values of n depend on the functional under consideration. For the corresponding n one may use single trajectories and take advantage of the effect of double randomization (if, e.g., the reactions take place in a random environment).

In the **first test case** $n = 1000$ is sufficient to resolve all four components of the solution. Even $n = 100$ provides reasonable results (cf. Table 1). Figure 8 allows us to conclude that in this situation the stochastic method needs less CPU-time than the deterministic method.

In the **second test case**, before ignition, one needs $n = 10^4$ to resolve the three components displayed in Figure 2. Results of single runs are given in **Figure 12**. Finally

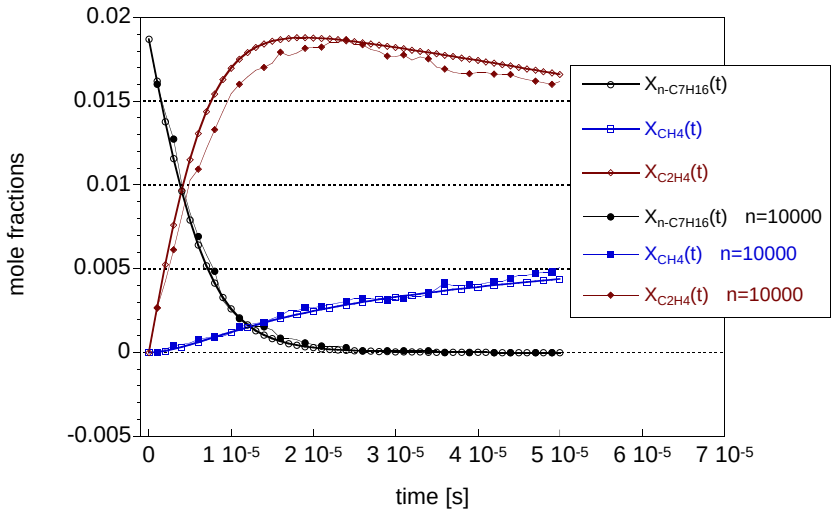

Figure 12: *Single run for the second test case (starting phase)*

we study the second test case on a time interval including the ignition point. A sufficient approximation of the mass density is obtained for $n = 10^4$. The corresponding results are given in **Figure 13** (cf. Table 3). However, after ignition, $n = 10^4$ is not enough to resolve all relevant components. The average curves for the component X_{OH} are given in **Figure 14**. Thus, one needs $n = 10^5$ in this example. **Figure 15** illustrates the behaviour of single trajectories.

Using Figure 9, we conclude that for $n = 10^4$ the stochastic algorithm is faster for simulation times up to 10^{-3}, while $n = 10^5$ it is faster only for simulation times up to 10^{-5}.

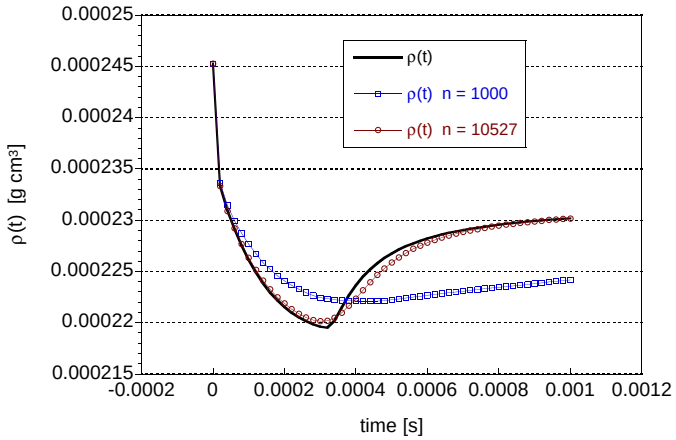

Figure 13: *Mean values for mass density in the second test case (after ignition)*

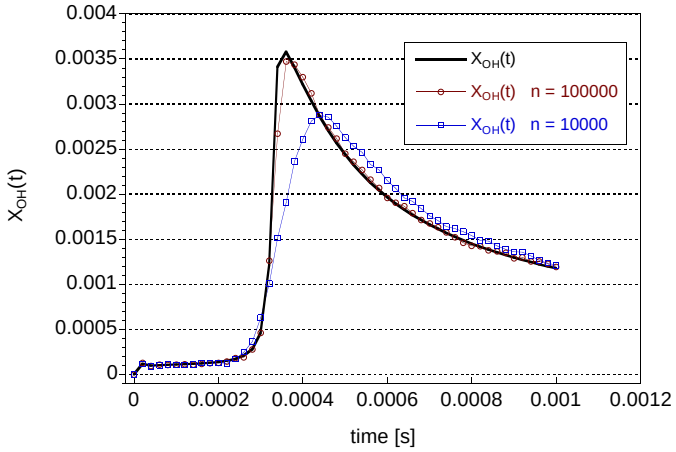

Figure 14: *Mean values for X_{OH} in the second test case (after ignition)*

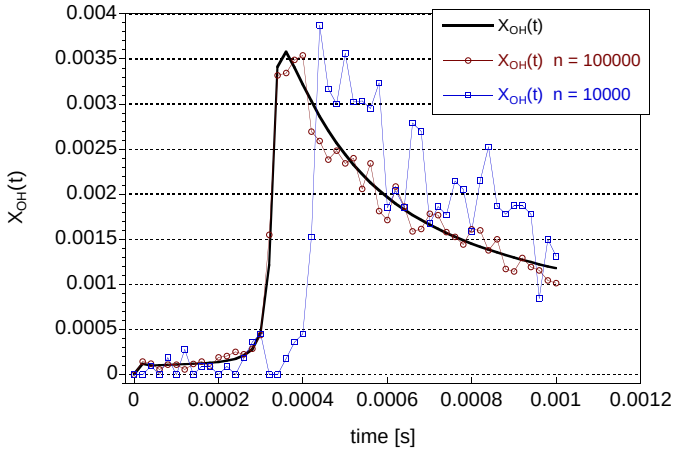

Figure 15: *Single run for X_{OH} in the second test case (after ignition)*

4. Concluding remarks

We have studied a stochastic particle method for homogeneous gas phase reactions. Convergence and performance properties of the stochastic algorithm were investigated systematically by comparing it with an efficient deterministic numerical method. It was demonstrated that the stochastic method can be successfully used for the numerical treatment of practically relevant problems, like the combustion of heptane that serves as primary reference fuel for internal combustion engines such as spark-ignition, diesel, and gas turbine engines. Chemical systems of this complexity have not been treated by this stochastic numerical method in the literature before.

The algorithm was described as a Markov jump process based on a particle number model. From this model the evolution equations of the deterministic quantities used to describe combustion problems have been derived. In the numerical examples, the systematic error of the method is found to be inversely proportional to the number of simulation particles. The issue of efficiency has been studied, and a comparison with an accurate deterministic method was performed. It turned out that in situations, where less accuracy is needed, the stochastic algorithm is much faster than the deterministic method. This problem was studied quantitatively, providing the dependence of the effort on the number of simulation particles.

In conclusion we mention two problems that are of considerable interest for further investigations. In order to evaluate the process of combustion of heptane correctly, we have to get radicals such as OH, H, O, H_2O_2 right during ignition. These components appear in very small concentrations or mole fractions. In the current algorithm a sufficient resolution can only be achieved by increasing the number of particles, which is time-consuming. Thus, the investigation of more general stochastic mechanisms of handling individual reactions is very promising. A second important point of practical relevance is to study stochastic algorithms for adiabatic systems.

Acknowledgments

One of the authors (MK) would like to thank the Weierstrass Institute for Applied Analysis and Stochastics, where most of the work was carried out, for hospitality and financial support. The assistance of I. Bremer and G. Telschow at computational issues is greatfully acknowledged.

Appendix:
Gillespie reaction mechanism in CHEMKIN format

```
!  Formal mechanism for CHEMKIN chemistry interpreter taken from
!  D.T. Gillespie, Journal of Computational Physics, 22, p.403-434, 1976
!  Example (33) on page 422.
!
ELEMENTS X/1/  END

SPECIES A B C D  END


!
!  Thermodynamic data taken from He
!
THERMO
A                 281095X   1               G  0300.00   5000.00  1000.00      1
 0.02500000E+02 0.00000000E+00 0.00000000E+00 0.00000000E+00 0.00000000E+00    2
-0.07453750E+04 0.09153489E+01 0.02500000E+02 0.00000000E+00 0.00000000E+00    3
 0.00000000E+00 0.00000000E+00-0.07453750E+04 0.09153488E+01                   4
B                 281095X   1               G  0300.00   5000.00  1000.00      1
 0.02500000E+02 0.00000000E+00 0.00000000E+00 0.00000000E+00 0.00000000E+00    2
-0.07453750E+04 0.09153489E+01 0.02500000E+02 0.00000000E+00 0.00000000E+00    3
 0.00000000E+00 0.00000000E+00-0.07453750E+04 0.09153488E+01                   4
C                 281095X   2               G  0300.00   5000.00  1000.00      1
 0.02500000E+02 0.00000000E+00 0.00000000E+00 0.00000000E+00 0.00000000E+00    2
-0.07453750E+04 0.09153489E+01 0.02500000E+02 0.00000000E+00 0.00000000E+00    3
 0.00000000E+00 0.00000000E+00-0.07453750E+04 0.09153488E+01                   4
D                 281095X   1               G  0300.00   5000.00  1000.00      1
 0.02500000E+02 0.00000000E+00 0.00000000E+00 0.00000000E+00 0.00000000E+00    2
-0.07453750E+04 0.09153489E+01 0.02500000E+02 0.00000000E+00 0.00000000E+00    3
 0.00000000E+00 0.00000000E+00-0.07453750E+04 0.09153488E+01                   4
!
!
!
REACTIONS    KCAL/MOLE
A     =>    B                                 1.0E-05    0.0  0.0E+00
B     =>    A                                 1.0E-05    0.0  0.0E+00
2A    =>    C                                 2.0E+00    0.0  1.0E+00
C     =>   2A                                 1.0E-05   -0.5  5.0E-01
A + D =>   2A                                 1.0E-00    0.0  1.0E+00
2A    =>   A + D                              1.0E-00    0.0  1.0E+00
END
```

References

[1] K. E. Brenan, S.L. Campbell, and L.R. Petzold. *Numerical Solution of Initial-Value Problems in Differential-Algebraic Equations*, volume 14. SIAM, Classics in Applied Mathematics, 1996.

[2] H.P. Breuer, J. Honerkamp, and F. Petruccione. A stochastic approach to complex chemical reations. *Chemical Physiscs Letters*, 190(3):199–201, 1992.

[3] H.P. Breuer, W. Huber, and F. Petruccione. Fluctuation effects on wave propagation in a reaction-diffusion process. *Physica D*, 73:259–273, 1994.

[4] H.P. Breuer, W. Huber, and F. Petruccione. The macroscopic limit in a stochastic reaction-diffusion-process. *Europhys. Lett.*, 30:69, 1995.

[5] D. L. Bunker, B. Garrett, T. Kleindienst, and G. S. Long III. Discrete simulation methods in combustion kinetics. *Combustion and Flame*, 23:373–379, 1974.

[6] H.J. Curran, P. Gaffuri, W.J. Pitz, and C.K. Westbrook. A comprehensive modeling study of n-heptane oxidation. *Combustion and Flame*, 114:149–177, 1998.

[7] D David, J.-P. Boon, and Yue-Xian Li. Lattice-gas automata for coupled reaction diffusion equations. *Physical Review Letters*, 66(19):2535–2538, 1991.

[8] S. N. Ethier and T. G. Kurtz. *Markov Processes, Characterization and Convergence.* Wiley, New York, 1986.

[9] M. Frenklach. Simulation of surface reactions. *Pure and Appl. Chem.*, 70:477–484, 1998.

[10] T. Fricke and J. Schnakenberg. Monte-Carlo simulation of an inhomogeneous reaction-diffusion system in the biophysics of receptor cells. *Z. Phys. B - Condensed Matter*, 83:277–284, 1991.

[11] D. T. Gillespie. A general method for numerically simulating the stochastic time evolution of coupled chemical reactions. *J. Comput. Phys.*, 22(4):403–434, 1976.

[12] D. T. Gillespie. Exact stochastic simulation of coupled chemical reactions. *J. Phys. Chem.*, 81:2340–2361, 1977.

[13] D. T. Gillespie. A rigorous derivation of the chemical Master equation. *Phys. A*, 188:404–425, 1992.

[14] W.D. Hinsberg and F.A. Houle. Chemical kinetics simulator 1.01, 1996. IBM Cooperation, http://www.almaden.ibm.com/st/.

[15] F.A. Houle and W.D. Hinsberg. Stochastic simulations of temperature programmed desorption. *Surface Science*, 338:329–346, 1995.

[16] W. Huber. Die Beschreibung von Reaktions-Diffusions-Prozessens durch Mastergleichungen. Master's thesis, University of Freiburg, Department of Physics, 1994.

[17] R.J. Kee, F.M. Rupley, and J.A. Miller. Chemkin-II: A fortran chemical kinetics package for the analysis of gas phase chemical kinetics. Technical report, Sandia Report SAND89-80009B UC-706, 1989.

[18] R. Kissel-Osterrieder, F. Behrendt, and J. Warnatz. Detailed modeling of the oxidation of CO on Platinium: A Monte-Carlo model. In *Twenty-Seventh Symposium (International) on Combustion*, 1998.

[19] T. G. Kurtz. The relationship between stochastic and deterministic models for chemical reactions. *J. Chem. Phys.*, 57(7):2976–2978, 1972.

[20] A.E. Lutz, R.J. Kee, and J.A. Miller. SENKIN: A fortran program for predicting homogeneous gas phase chemical kinetics with sensitivity analysis. Technical report, Sandia Report SAND87-8248 UC-401, 1988.

[21] A.S. McLeod and L.F. Gladden. A Monte Carlo study of temperature-programmed desorption from supported-metal catalysts. *Catalysis Letters*, 55:1–6, 1998.

[22] U. Wetterauer, J. Knobloch, P. Hess, and F.A. Houle. In situ fourier transform infrared spectroscopy and stochastic modeling of surface chemistry of amorphous silicon growth. *Journal of Applied Physics*, 83(11):6096–6105, 1998.